Technical Note

ISSN 1997-1400 Int. J. Pavement Res. Technol. 2(5):231-235

Combining Strain Measurement and FEM Simulation to Obtain Dynamic Response of Asphalt Pavement

Zejiao Dong[1+], Yiqiu Tan[2], Liping Cao[3+], and Hao Liu[4]

Abstract: Obtaining asphalt pavement strain response plays an important role in understanding pavement damage mechanisms in structural design and in predicting the life of the pavement. Combining strain measurement and finite element simulation is crucial to identifying whether or not the measured strain reflects the actual mechanical state. Therefore, the viscoelastic characteristics of asphalt mixtures were obtained first using a dynamic modulus test. Then, a small-scale laboratory loading test was developed according to the similarity theory with Fiber Bragg Grating (FBG) sensors embedded. Studies were then carried out to validate the measured strains in conjunction with a finite element method (FEM) model using the same conditions as in ABAQUS software. Finally, a brief description of the on-site instrumentation was introduced, followed by a preliminary analysis of typical three directional strain responses.

***Key words**: 3D FEM simulation; Asphalt pavement; Dynamic response; FBG sensor; Moving loading; Viscoelastic characteristics.*

Introduction

In recent years, premature failures, such as rutting, stripping, and cracking, have been observed frequently in asphalt pavements in China. In order to identify the mechanisms of these failures, it is of significant importance to obtain the dynamic response data on pavements subjected to the traffic loading in actual pavements. The Fiber Bragg Grating (FBG) sensor is a comparatively promising new type of sensor that monitors the actual strain of pavement structure during long-term service. Compared with conventional sensors used in pavements, the FBG sensor has many advantages [1]:

- High precision - it has a temperature sensitivity rate of 10pm/°C, and a strain sensitivity rate of 1.2pm/$\mu\varepsilon$. The resolution of the fiber demodulator is 1pm. That is to say, the sensitivities of the temperature and strain measurements are 0.1°C and 0.83$\mu\varepsilon$, respectively. Furthermore, the sampling frequency of the fiber demodulator can reach 250Hz, or even 1,000Hz, which is good enough to catch the dynamic pavement response of high-speed vehicular traffic with high precision.
- Absolute measurement - an important advantage of the FBG sensor is its ability to measure an absolute value of a variable such as strain or temperature due to its self-referencing capability in the wavelength domain; it thus has a distinct advantage over other traditional sensors by obtaining both static and dynamic pavement response.
- Immunity to corrosion - the chief component of the fiber core is silicon dioxide, which is very stable in acid or alkaline conditions.
- Immunity to electromagnetic interference and electrical hazards - FBG sensors transfer signals using optical waves, and an optical fiber does not conduct electrical current, so the signals cannot be influenced by electromagnetic fields and also do not influence exterior electromagnetic fields.

As a result, the development and application of FBG sensors for pavement monitoring is spreading rapidly [2-6]. However, it is difficult to identify whether the measured strains obtained on site reflect the actual mechanical state as there is an interaction between pavement material with viscoelastic characteristics and strain sensors with high modulus [7]. Therefore, combining strain measurement with FBG sensors and finite element method (FEM) simulation to obtain a reasonable pavement response is important.

Viscoelastic Characterization of Asphalt Mixture

The viscoelastic properties of the asphalt mixtures were determined using the dynamic modulus test procedure contained in the National Cooperative Highway Research Program (NCHRP) Report 465 [8] for determining the permanent deformation of asphalt concrete mixtures. The UTM-100 testing apparatus was used to apply a sinusoidal force on the test specimens. After an initial preconditioning, the selected dynamic load was applied to the specimen, and the axial deformation measured by the extensometers. Measurements were recorded at frequencies of 25, 10, 5, 1, 0.5 and 0.1Hz. Each specimen was tested at temperatures of -10, 4.4, 21.1, 37.8, and 54.4°C.

For typical viscoelastic materials like asphalt aggregate mixtures, the effects of time and temperature can be expressed using the shift factor. By taking measurements at different loading times and temperatures, these measurements can be used to construct a master curve of relaxation modulus as a function of reduced time [9]. Fig. 1 shows the relaxation modulus master curve determined in the laboratory using a reference temperature of 21.1°C.

[1] Associate Professor, School of Transportation Science and Engineering, Harbin Institute of Technology, Harbin 150090, China.
[2] Professor, School of Transportation Science and Engineering, Harbin Institute of Technology, Harbin 150090, China.
[3] Assistant Professor, School of Transportation Science and Engineering, Harbin Institute of Technology, Harbin 150090, China.
[4] Professorate Senior Engineer, School of Transportation Science and Engineering, Harbin Institute of Technology, Harbin 150090, China.
[+] Corresponding Author: E-mail hitdzj@hit.edu.cn
Note: Submitted September 27, 2008; Revised March 28, 2009; Accepted May 27, 2009

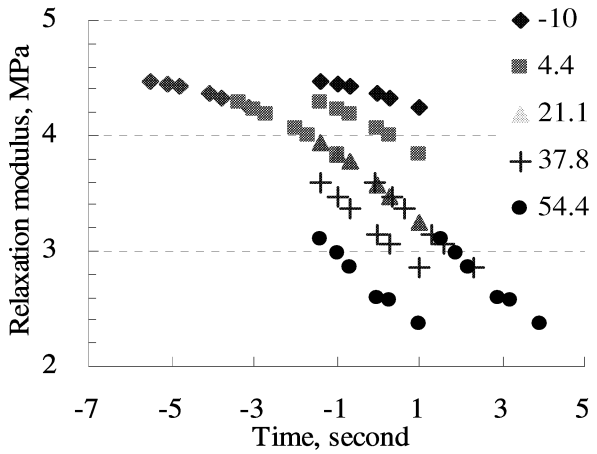

Fig. 1. Relaxation Modulus and Master Curve (Log-Log Scale).

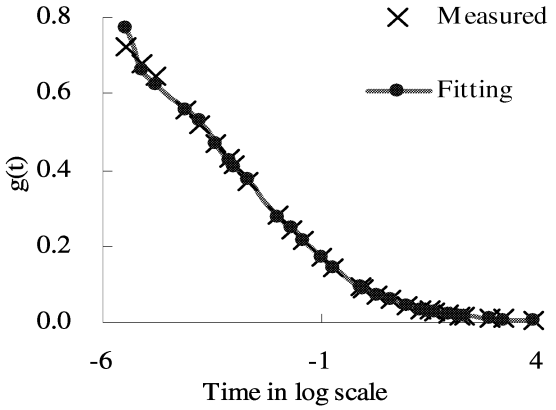

Fig. 2. Comparison of the Measured and Calculated g_i.

To describe the time dependency of a viscoelastic material in ABAQUS, it is generally accepted that a Prony series expansion is adequate:

$$g(t)=1-\sum_{i=1}^{N} g_i\left(1-e^{(-t/\tau_i)}\right) \quad (1)$$

where, $g(t)$ is computed by normalizing $G(T)$ by G_0 (the instantaneous shear modulus); N is the number of Prony series terms; g_i is the Prony series coefficient; and τ_i is the retardation time. The shear modulus, $G(T)$, can be calculated from the relaxation modulus $E(t)$ as follows:

$$G(t)=\frac{E(t)}{2(1+\mu)} \quad (2)$$

where, μ is the Poisson's ratio, assumed to be 0.35 over the range of test temperatures and loading frequencies in this study.

To obtain the Prony series in Eq. (1), a series of retardation times τ_i, were assumed to cover the range of testing. Next, the linear least squares curve fit was used to find the coefficients of the Prony series. Here, 10 Prony series terms are used to obtain a sufficiently accurate approximation to the laboratory-determined data. The comparison of measured and calculated g_i is shown in Fig. 2.

Validation of Measured Strain through a Small-Scale Loading Test

Small-Scale Loading Tests

Before in-situ measurements in an actual road were implemented, the validation of the data collected from the FBG strain sensors is important and critical. This is essential to the successful implementation of in-situ monitoring of measured data and data analysis on site. Therefore, a validation test was undertaken in the laboratory. In comparison with a full-scale Accelerated Loading Facility, data may suffer from boundary effects while it is preponderant due to its accessibility and its full-controlled environment.

The wheel tracking test was modified to develop a Small-Scale Loading Test (SSLT). The surface dimensions of the SSLT specimen for one layer of asphalt mixture was 0.3m by 0.3m, and the thickness was 0.18m. The loading contact area was 0.048m long and 0.018m wide. These sizes were obtained assuming that the geometric similarity between the in-situ measurement conditions and those of the laboratory is 10 according to the Similarity Theory [10]. The specimen was compacted using a rolling compactor to a density comparable with that obtained in the dynamic modulus test. The strain sensor was installed at the depth of 0.03m. When the SSLT was running, the transient strain history from the embedded sensor was recorded through an Optical Sensing Interrogator. Fig. 3 shows selected pictures taken during the experiment in laboratory.

Validation with Finite Element Simulation

A three-dimensional finite element (FE) model was developed using ABAQUS to simulate the SSLT. The analysis simulated a wheel

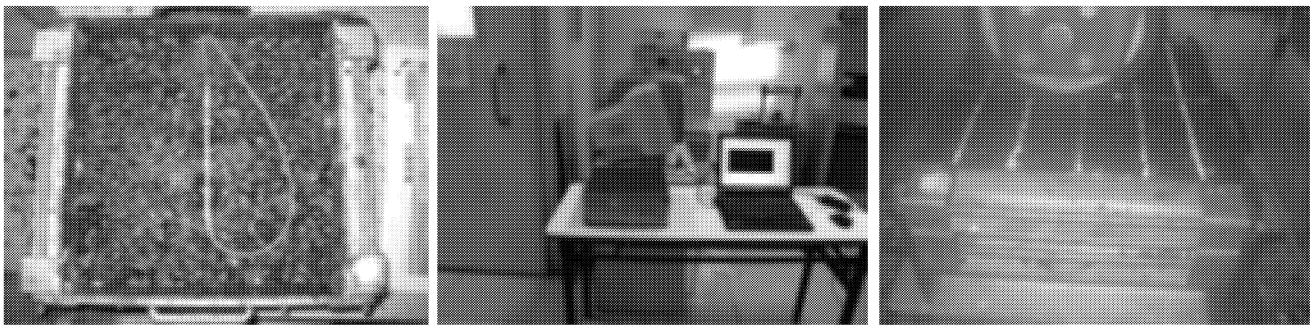

Fig. 3. The Installation of FBG Sensors and Data Collection.

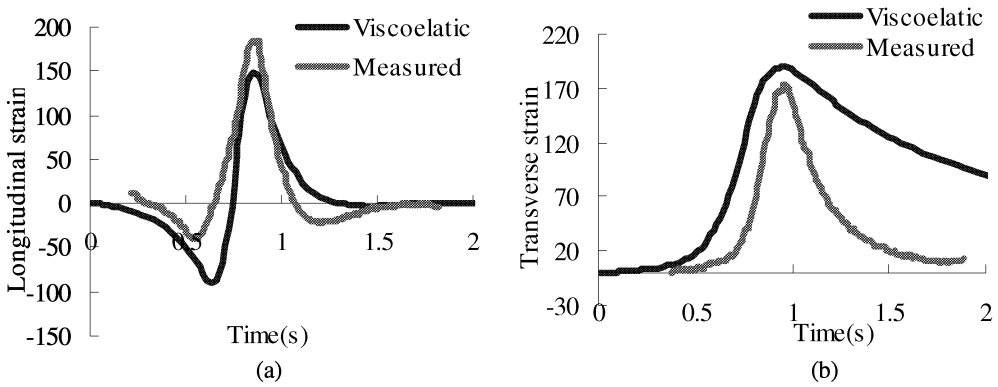

Fig. 4. The Strain Histories at the Depth of 0.03*m*: (a) Results at 60℃, (b) Results at 20℃.

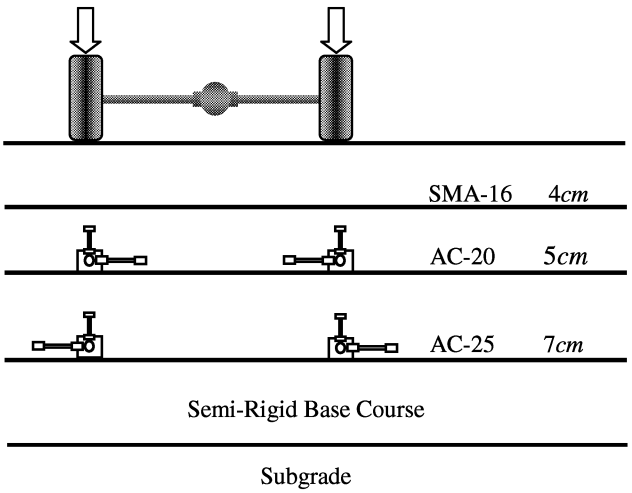

Fig. 5. Locations of FBG Strain Sensors for One Section (Not Drawn to Scale).

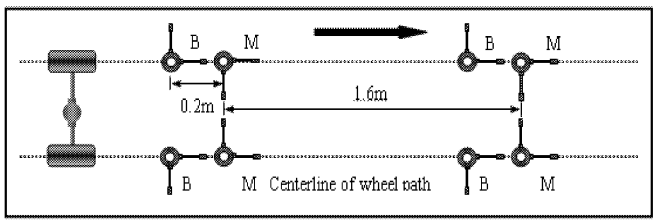

Note: "B" Denotes in Bottom Asphalt layer; "M" Denotes in Middle Asphalt Layer.

Fig. 6. Layout Scheme of Strain Sensors for Testing Segment (Not Drawn to Scale).

travelling at a constant speed at a contact pressure of 0.7*MPa*. The dimensions of the model were 0.3*m* by 0.3*m*, the same as the tested specimen. No symmetry was considered in the model developed. The mesh used was designed to reduce calculation time and obtain good accuracy (fine mesh was used in the loading area of the specimen and coarse mesh at the two ends). Eight-node linear brick reduced integration elements (C3D8R) were chosen.

Naturally, the wheel applies a moving dynamic loading to the specimen, thus wheel loading should be considered as a dynamic moving load in the FE model. To simulate the movement of loading, the load area of each footprint was gradually shifted along the wheel path in the direction of movement. For each load area, the amplitude of the loading waveform was represented by a trapeze form function. The loading was moved a distance of 0.04*m* (four elements in transverse direction) in each increment, thus the load time can be calculated by dividing the distance by the wheel speed. In total, up to 48 increments (locations of the loading) were used to achieve one full passage of the wheel over the entire model.

It was assumed that there was no vertical, transverse, or longitudinal movement at the bottom of the FE model, thus the bottom of the model was completely restrained. Horizontal movement perpendicular to the perimeters was also restrained; whereas the remaining two directions were considered free (thus there were two degrees of freedom). Since the specimen comprised of three layers compacted within a short interval, the interface between the different layers was assumed to be tied together without any relative movement. Fig. 4 shows examples of the comparison between the measured and simulated longitudinal strain and transverse strain at a temperature of 60℃.

As can be seen from Fig. 4(a), the calculated longitudinal strain has a lower positive value and a higher negative value than the measured strain. However, the amplitude from the positive to the negative value of the calculated longitudinal strain is comparable with that of the latter at about 4.3%. As for the transverse strain, the calculated value is higher than the measured value at about 9.7%. It is also observed that the duration time of the simulation is obviously longer than the measured time. Moreover, the residual strain is higher than that of the latter. Through a carefully analysis, a factor should be considered that only one passage is applied to the viscoelastic specimen in the simulation. That is to say, there is no densification course compared with the small-scale loading test. Generally, the measured strain matches the simulated model, which indicates that the FBG sensor can be used in the actual in-situ measurement.

Instrumentation

Fig. 5 shows the on-site scheme for the installation of the strain sensors through the depth of the asphalt pavement. A total of 24 strain sensors were installed in pavement; these were divided into eight groups. Each group sensor was used to measure the longitudinal, transverse, and vertical strain, respectively (three sensors were jointed with a nylon junction). Two similar sections

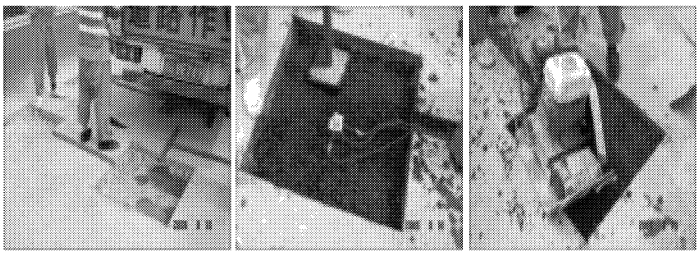

Fig. 7. Installation of FBG Strain Sensors on Site.

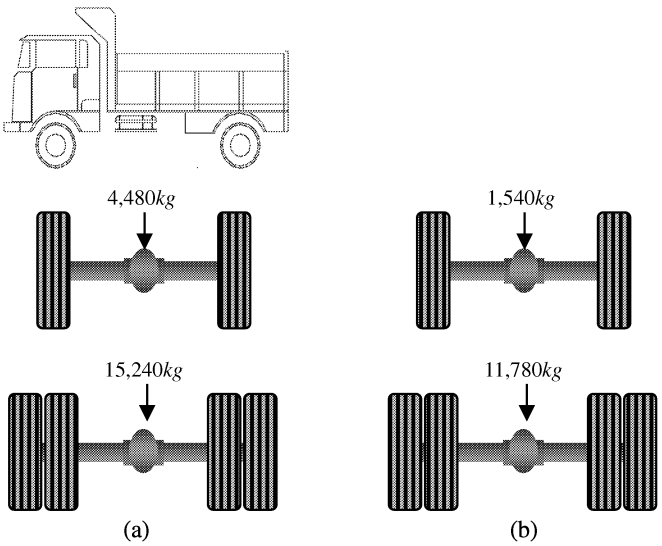

Fig. 8. Two Loading Levels for Strain Measurements (a) Loading Level I and (b) Loading Level II.

Fig. 9. Strain Response Measurement on Site.

within a distance of 1.6*m* were used to make sure that proper strain measurements were obtained. Two groups were located at the bottom of the middle asphalt layer under the two wheel paths. Another two groups were installed at the bottom of the bottom asphalt layer with a horizontal distance of 0.2*m* from the upper groups as shown in Fig. 6. Four FBG temperature sensors were installed in the pavement shoulder at the same depth as the strain sensors in order to take into account the temperature effect on the measured strains.

Because the strain measurements were performed after the asphalt pavement was built, the proper cutting area is important in order to minimize the disturbance at the boundary area between the existing material and the embedded sensors.

To do this, a 0.8*m* by 0.8*m* planer section was milled and filled with the same pavement material as the original pavement. The installation of strain sensors is shown in Fig. 7.

All of the in-situ strain sensors were tested before and after installation to ensure proper data collection. The strain responses were measured under various loading conditions. Fig. 8 shows the axle components of two trucks used in the experiment. The truck speeds were varied from 5 to 20*km/h*. An SI 425 Optical Sensing Interrogator whose frequency was 250Hz was used to collect the signals from the sensors. Fig. 9 gives the in-situ strain measurement conditions.

Results and Analysis

Concerning the time histories from the strain sensors, it was found that the shapes of the responses from most of the sensors and loading cases were always similar. Fig. 10 shows a typical three directional strain history from the middle asphalt layer recorded during the passing of the rear axle at load level II of a testing truck travelling at a speed of 10.9*km/h*. It can be seen that in the longitudinal direction, the sensor first shows compressive strains from the approaching load, then significant tensile strains during passing of the load, and finally, compressive strain when the load moves away. There is an observable gradual recovery of residual strain after the load passes. Generally, the pavement material is alternatively submitted to compressive and tensile strains.

In contrast, in the transversal direction, the sensor shows a small compressive strain from the approaching load, and then significant tensile strains are observed during the passing of the loading. As for the vertical direction, a small tensile strain is seen when the loading is approaching, and a primary compressive strain is recorded during the passing of the load. Moreover, similar to the longitudinal direction, an observable residual strain also exists and recovers step-by-step when the load leaves. The strain remaining in longitudinal and vertical directions illustrate that asphalt pavement shows viscoelastic characteristics when an external traffic loading is applied.

Conclusions and Further Recommendations

This paper gives preliminary results from a study of one expressway in China using FBG strain sensors developed by the Harbin Institute of Technology. This paper presents details on the viscoelastic characterization of an asphalt mixture, validation of FBG sensors data by small-scale load testing in the laboratory, instrumentation on-site, and the results of general observations of strain measurements. It is noted that no vertical strain measurements as presented in this paper are available in published data.

From the results of these strain measurements in China, it can be seen that three directional strain measurements can reflect a good response at different depths within pavement structure and at different loading conditions as defined by the experiment. It is acknowledged that the strain measurements reported here are all classified as single-point strain measurement, not distributed ones. Therefore, it is important to try to control the testing conditions as designed, such as loading position, speed, and magnitude, etc., as the response evidently depends on the loading conditions.

The numerical simulation of the complicated distribution of moving loads on an asphalt pavement based on in-situ material characteristics has been carried out. Further comparison studies between simulation and on-site measurement and performance

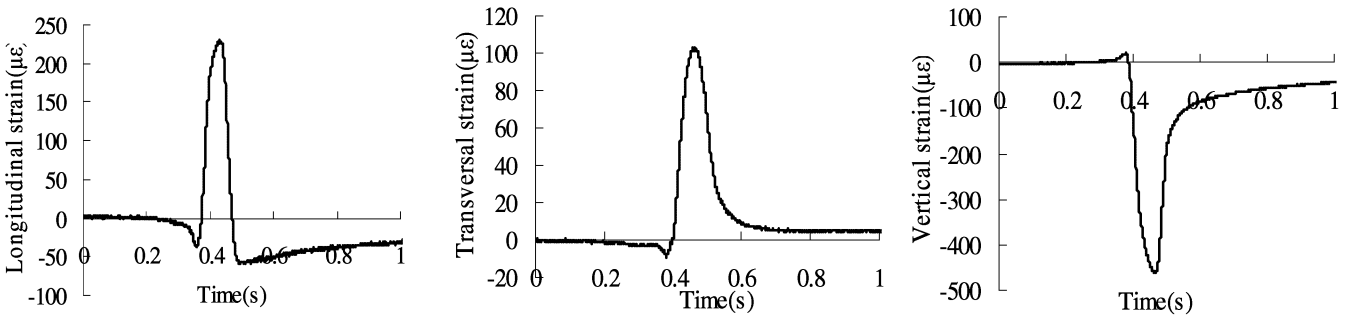

(a) (b) c)

Fig. 10. Typical Three Directional Strain Response Histories: (a) Longitudinal Strain History (b) Transverse Strain History, and (c) Vertical Strain History.

evaluation of asphalt pavements based on the measured strains are recommended.

Acknowledgements

The work presented herein was the result of hard work by many people. The authors would like to express their gratitude to Beijing Municipal Road & Bridge Holding Company for their effort in sensors installation and data collection. The authors are also grateful for funding from the National Natural Science Foundation of China (50808056), Specialized Research Fund for the Doctoral Program of Higher Education (SRFDP) for Young Teachers (20070213014), and Development Program for Outstanding Young Teachers in Harbin Institute of Technology (HITQNJS.2007. 032).

References

1. Li, J.S., (2007). Development and Performance of Asphalt Pavement Strain Sensors Based on FBG Technology, *Master Science Thesis*, Harbin Institute of Technology, Harbin, China.
2. Wulf von Eckroth, (1999). Development and Modelling of Embedded Fiber-Optic Traffic Sensors, *Ph.D. Dissertation*, Florida Institute of Technology, USA.
3. Miller, C.E., (2000). Development of a Fiber Optic Pavement Subgrade Strain Measurement System, *Ph.D. Dissertation*, University of Maryland, USA.
4. Cosentino, P.J., Wulf von Eckroth, and Grossman, B.G., (2003). Analysis of Fiber Optic Traffic Sensors in Flexible Pavements, *Journal of Transportation Engineering*, 129(5), pp. 549-557.
5. Wang, J.N., Tang, J.L., and Chang, H.P., (2006). Fiber Bragg Grating Sensors for Use in Pavement Structural Strain-Temperature Monitoring, *Smart Structures and Materials 2006: Sensors and Smart Structures Technologies for Civil, Mechanical, and Aerospace Systems, Proc. of SPIE, 6174(2)*, pp. 61743S.1-61743S.12, Harbin, China.
6. Galal, K., Sharp, S.R., and Elfino, M.K., (2007). Fiber-Optic Sensors Strain Measurements under an Asphalt Layer During and After Construction, *TRB 2007 Annual Meeting*, CD-ROM, Washington DC, USA.
7. Zafar, R., Nassar, W., and Elbella, A., (2005). Interaction between Pavement Instrumentation and Hot-Mix-Asphalt in Flexible Pavements, *Emirates Journal for Engineering Research*, 10(1), pp. 49-55.
8. National Cooperative Highway Research Program (NCHRP) Report 465, (2002). Simple Performance Test for Superpave Mix Design: Appendix A–Test Method for Dynamic Modulus of Asphalt Concrete Mixtures for Fatigue Cracking, *NCHRP Report 465*, Transportation Research Board, National Research Council, Washington DC, USA.
9. Liao, Y., (2007). Viscoelastic FE Modelling of Asphalt Pavements and Its Application to U.S. 30 Perpetual Pavement, *Ph.D. Dissertation*, the Russ College of Engineering and Technology, USA.
10. Cheng, X.L., (2008). Research on the Wheel Tracking Test Based on Similarity Theory and Finite Element Simulation, *Master Science Thesis*, Harbin Institute of Technology, Harbin, China.